Title

M 450-Mev/c K- AND p BEAMS AT THE NORTHWEST TARGET AREA OF THE BEVATRON SEPARATED BY THE COAXIAL VELOCITY SPECTROMETER

Authors

Horwitz, Nahmin
Murray, Joseph J.
Ross, Ron R.
et al.

Publication Date

1958-06-01

UNIVERSITY OF CALIFORNIA

Ernest O. Lawrence Radiation Laboratory

BERKELEY, CALIFORNIA

DISCLAIMER

UCRL-8269
Physics and Mathematics

UNIVERSITY OF CALIFORNIA

Radiation Laboratory
Berkeley, California

Contract No. W-7405-eng-48

450-Mev/c K^- AND $\bar{p}$ BEAMS AT THE NORTHWEST TARGET AREA OF THE BEVATRON SEPARATED BY THE COAXIAL VELOCITY SPECTROMETER

Nahmin Horwitz, Joseph J. Murray, Ron R. Ross, and Robert D. Tripp

June 1958

Printed for the U. S. Atomic Energy Commission

450-Mev/c K^- AND $\bar{p}$ BEAMS AT THE NORTHWEST TARGET AREA OF THE BEVATRON SEPARATED BY THE COAXIAL VELOCITY SPECTROMETER

Nahmin Horwitz, Joseph J. Murray, Ron R. Ross, and Robert D. Tripp

Radiation Laboratory
University of California
Berkeley, California

June 1958

Abstract

Enriched beams of 450-Mev/c K^- mesons and antiprotons have been produced by separation with the coaxial static electromagnetic velocity spectrometer. Characteristics of the final separated beams as observed in the 15-inch hydrogen bubble chamber are given together with a detailed description of the beam optics and apparatus.

450-Mev/c K^- AND $\bar{p}$ BEAMS AT THE NORTHWEST TARGET AREA OF THE BEVATRON SEPARATED BY THE COAXIAL VELOCITY SPECTROMETER

Nahmin Horwitz, Joseph J. Murray, Ron R. Ross, and Robert D. Tripp

Radiation Laboratory
University of California
Berkeley, California

June 1958

The beams referred to are in fact the same beam, arising from a copper target in the Bevatron proton beam, with the coaxial spectrometer[1] set to transmit either K^- or $\bar{p}$. In Fig. 1 is a schematic diagram of the complete system. In Fig. 2 are shown the over-all characteristic curves of the spectrometer,[2] with operating points indicated for this particular application. Table I lists values of the significant parameters of each of the other elements of the system.

Characteristics of the final separated beams, as observed in the 15-inch hydrogen bubble chamber with enough absorber to stop the desired particles in the chamber, are as follows (containment of the desired particles in the visible range interval presented by the chamber was essentially 100%):

Momentum spread: ± 2%

Beam size: 5 in. horizontal by $1\frac{1}{2}$ in. vertical at center of bubble chamber, 25 in. beyond final collimator (C_2)

Virtual source in horizontal plane: $\frac{1}{2}$-in. slit at final collimator

Virtual source in vertical plane: at ∞ with ± 0.01 radian angular limits

Dispersion: essentially no correlation between position and momentum

Total background tracks per stopped K^- 65 : 1

---

[1] Joseph J. Murray, A Coaxial Static-Electromagnetic Velocity Spectrometer for High-Energy Particles, UCRL-3492, May 1957.

[2] The radial equation of motion in the spectrometer for particles coplanar with the spectrometer axis is

$$d^2\rho/dz^2 = F\,(\rho_0/\rho) = [(E/\beta - H)/p]\,(\rho_0/\rho)\ ,$$

where ρ is the radial coordinate, p is momentum, and E and H are the field intensities at the inner conductor radius, ρ_0. Thus we have $F = (E/\beta - H)/p$, and at a certain value F_π the inner envelope of the trajectories of pions emerging from the spectrometer just excludes the exit aperture. That is, the value of $F = F_\pi$ satisfies the criterion for rejection. At the same time F_π serves as a convenient unit to describe the spectrometer forces in any situation. Optimum transmission, for example, occurs for $F/F_\pi \approx 0.2$. The straight lines in Fig. 2 are the loci of values of E and H for $F/F_\pi = 1$ for pions at the various momenta indicated and for entrance- and exit-aperture diameters of 4 inches and 3 inches, respectively.

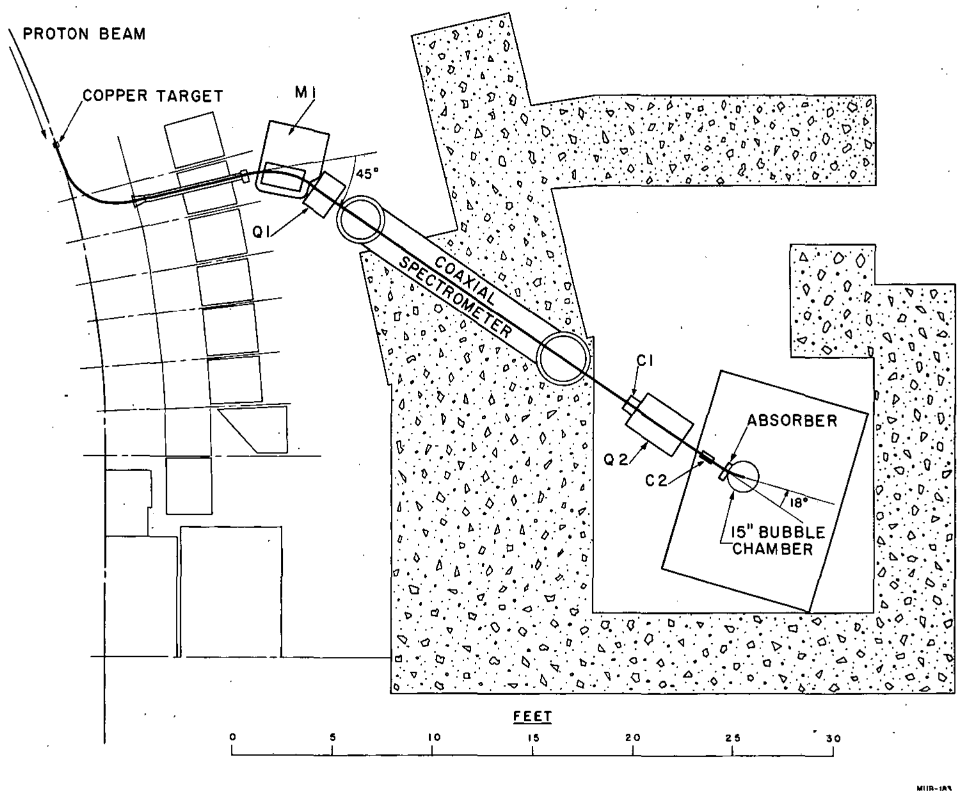

Fig. 1. Schematic diagram of the system.

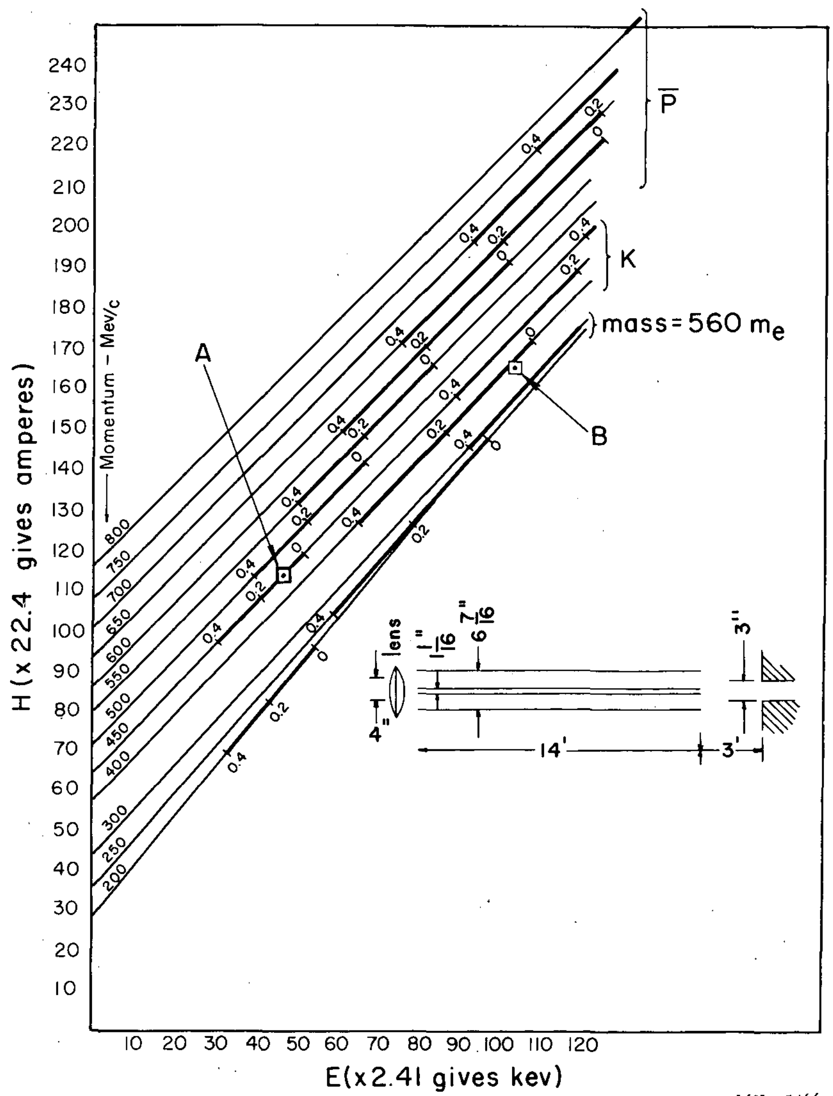

MU-15466

Fig. 2. Characteristics of a Coaxial Static Electromagnetic Velocity Spectrometer. Heavy portions of momentum contours are the useful operating regions for particles indicated. Rejected particles are pions. The appended numbers are ratios of the force constants of the selected particles and pions. This ratio determines the proper image distance for the entrance lens. A: 450-Mev/c $\bar{p}$; 112 kev; 2530 amp; $(F/F_\pi)_\pi = 1.0$; $(F/F_\pi)_{\bar{p}} = 0.1$; 3.5-inch diam. entrance and exit apertures, B: 450-Mev/c K^-; 250 kev; 3700 amp; $(F/F_\pi)_\pi = 0.88$; $(F/F_\pi)_K = 0.17$; 3.5-inch diam entrance and exit apertures.

Table I

Significant parameters of each of the elements of the system

Element	Description	Currents
Target	Copper, $3\frac{1}{2} \times \frac{1}{2} \times \frac{1}{2}$ inches Flipped azimuthally Radius $597\frac{1}{2}$ inches Azimuth 72° 29' Momentum 450 Mev/c at I pip 33 + 5 msec Target angle ≈ 0°	----
Bevatron exit window	0.008-inch aluminum	
Helium bag	0.00025-inch polyethylene. Ends, 40" long in M1	
M1	General Electric C Magnet	
	Pole tips MK I (see Magnet Testing Book 294, Joe Dorst)	870 amp
	Pole tips MK II (see Engr. Note 7910-55 MT-2, Apr. 18, 1958, L. G. Ratner)	694 amp
Q1	Single 4 in.-diam quadrupole	With MK I pole tips in M1: 30 amp
	Vertical plane: defocusing Horizontal plane: focusing	With MK II pole tips in M1: 40 amp
	Filled with brass collimator 1 foot long, 3.5 in. inside diameter	
Spectrometer entrance window	0.005-inch aluminum	
Spectrometer	See Fig. 2 for operating points See UCRL-3492 for general description See Engr. Note 7307-01 M23, Feb. 27, 1958, R. A. Kilpatrick for design data	
Spectrometer exit window	0.020-inch aluminum	

Table I (continued)

C1	Brass collimator, 1 foot thick, 3.5-inch inside diam, 9 $\times$ 9 inches outside dimensions	
Q2	Two-element 4-in.-diam quadrupole 8-in.-long sections spaced 7.5 in. Vertical plane: focusing - defocusing Horizontal plane: defocusing - focusing	Section near spectrometer: 210 amp Section near bubble chamber: 380 amp
C2	Copper collimator with uranium slit jaws Plan: 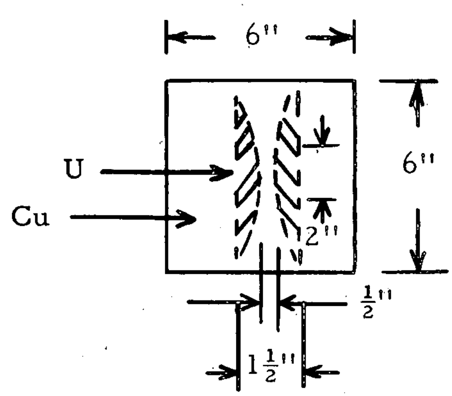 Elevation in beam direction: 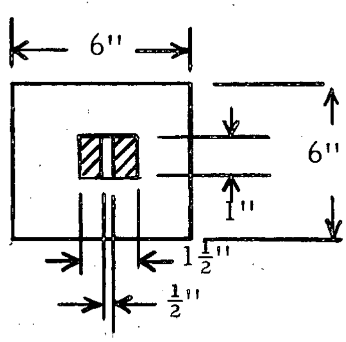 Center located 21½ in. beyond end of pole tip of final section of Q2	
Absorber	For stopping K^- in bubble chamber: For stopping $\overline{p}$ in bubble chamber:	1.62 in. Cu, 35 g/cm^2 1/16 in. Cu

Table I (continued)

Bubble-chamber window	1/4 in.-stainless steel, 4.9 g/cm^2 Cu equivalent

Stopped K^- per 10^{10} protons on target	1 : 4
Total background tracks per stopped $\overline{p}$	4000 : 1
Stopped $\overline{p}$ per 10^{10} protons on target	1 : 250
Background constitution: ~ 85% μ (and e ?), ~ 15% π	
Ratio of particle fluxes in chamber with separator off and on (definition of "rejection ratio")	700 : 1

A momentum distribution of background tracks observed in the bubble chamber is shown in Fig. 3. If this distribution could be separated into muon and pion components, one would expect, on the basis of background calculations mentioned in an earlier report,[1] to find two fairly well defined groups of muons at ~ 450 Mev/c and 260 Mev/c (in a ratio of approximately 9:1) whereas the pion component would be broadly distributed over the full range of momenta.

The pion content of the background was determined by comparison of the observed cross section of background particles for production of π-p interactions with a "known" π-p cross section. The result, 15%, is consistent with the expected pion content, but is uncertain by a factor of about 2 because of the very uncertain momentum distribution of the background pions.

The nature and sources of the background, and the role of the rear-end optical system, which consists of Q2 and of the collimators C1 and C2 ahead of and following Q2, are as follows:

The transmitted beam arriving at collimator C1 (just ahead of Q2) forms a slightly elliptical, ring-shaped image, as indicated by the beam profiles in Fig. 4. It has an angular distribution largely contained between directions paraxial and divergent by 0.01 radian. (The spectrometer optics is such that a representation of its effect in terms of a virtual source for Q2 is not particularly useful.) In order to accept this beam, the final collimator C2 (following Q2) is adjusted to present an angular aperture ahead of Q2 of ± 0.01 radian.

The muon contamination at this same point has a fairly uniform angular distribution over a range much greater than 0.01 radian but including the paraxial direction. Hence some of the muon contamination is necessarily accepted, and the component having full momentum constitutes a minimum background reducible only by further velocity analysis.

When the spectrometer is operated in a condition corresponding ideally to complete rejection of pions (this means no possible pion trajectories that connect the entrance and exit apertures directly), the pion contamination consists only of (a) π mesons scattered out of the collimator ahead of Q2, and (b) those scattered in from the outer conductor. With increasing rejection force (a) should decrease, (b) should increase, and (a) should be much more sensitive than (b). The pion background as a function of rejecting force should therefore exhibit a minimum, and at the minimum should consist mainly of π mesons scattered in from the outer conductor. The observed background indeed has a minimum, which occurs at a rejecting force approximately equal to the ideal minimum value (see Figs. 5 and 6).

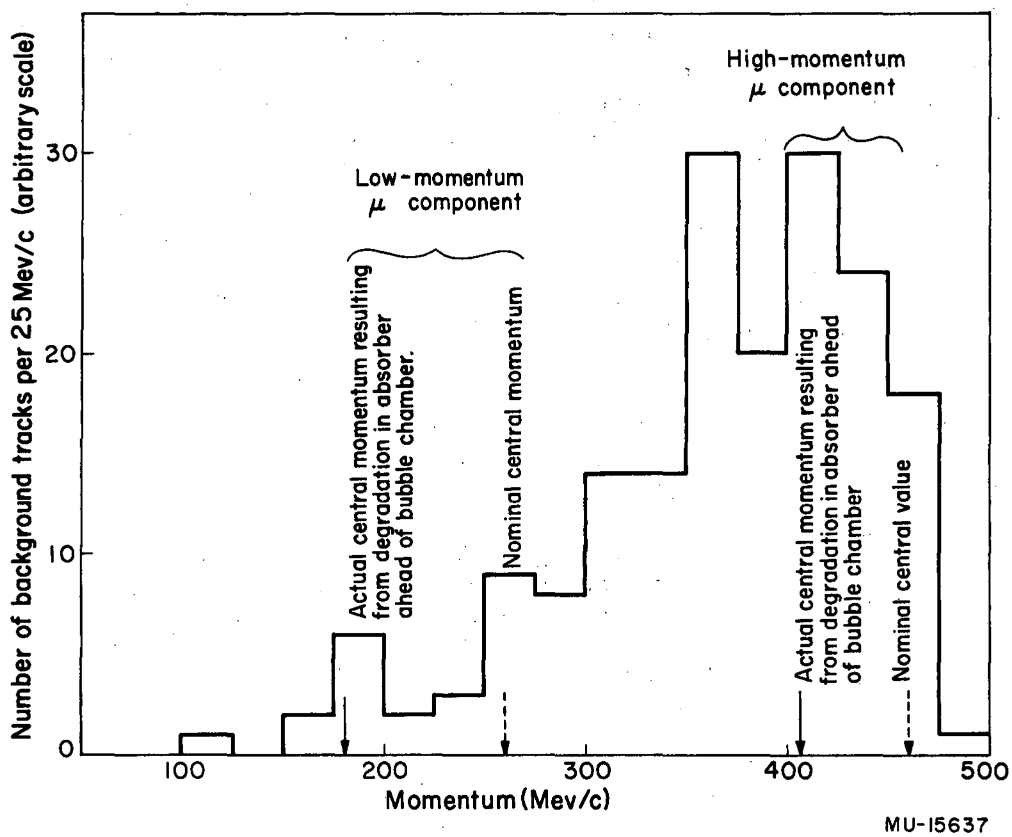

Fig. 3. Momentum distribution of background particles observed in bubble chamber with 35 g/cm^2 of Cu absorber ahead of bubble chamber. The high- and low-momentum μ components result from π-μ decays in which the μ is almost forward and almost backward, respectively, in the center-of-mass frame. Because of the limited angular acceptance of the rear-end optics only these distinct components are expected to appear in the background, and should occur in a ratio ~9:1 respectively. In addition the background contains an estimated 15% pion component broadly distributed in momentum.

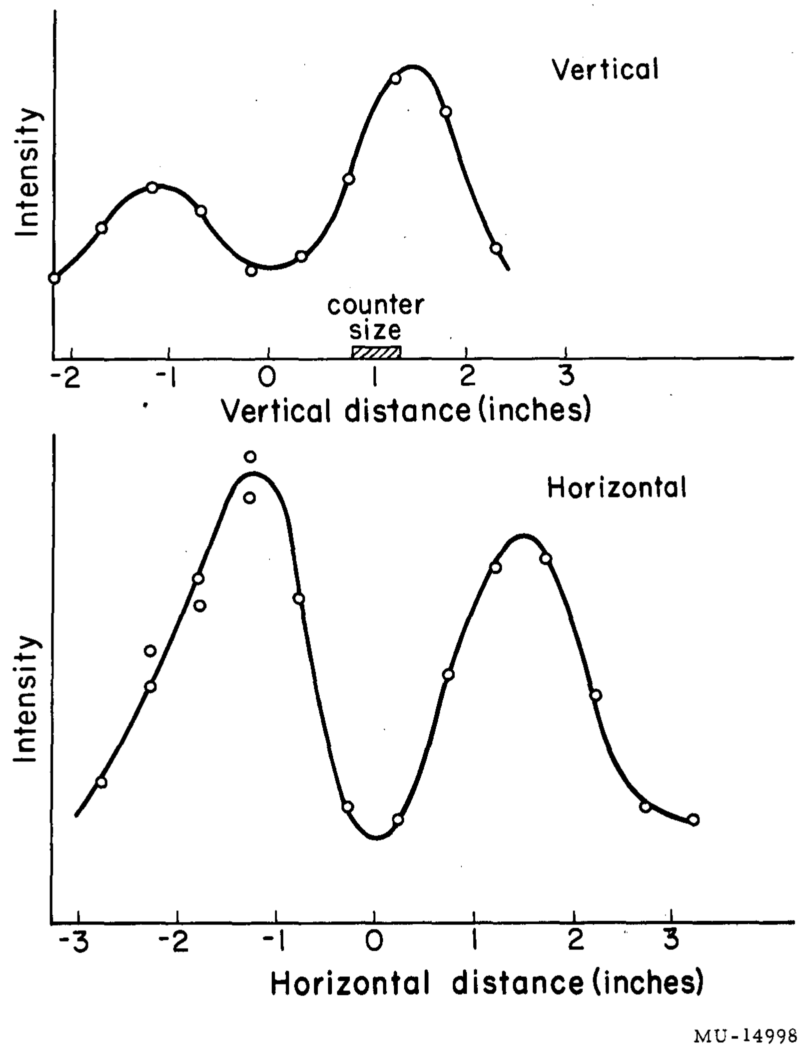

Fig. 4. Vertical and horizontal beam profiles 3 feet beyond spectrometer (just ahead of collimator). $F/F_\pi = 0.2$. Total flux integrated over 3-in.-diam central area was $15 \times 10^3\ \pi/10^{10}$ protons on target.

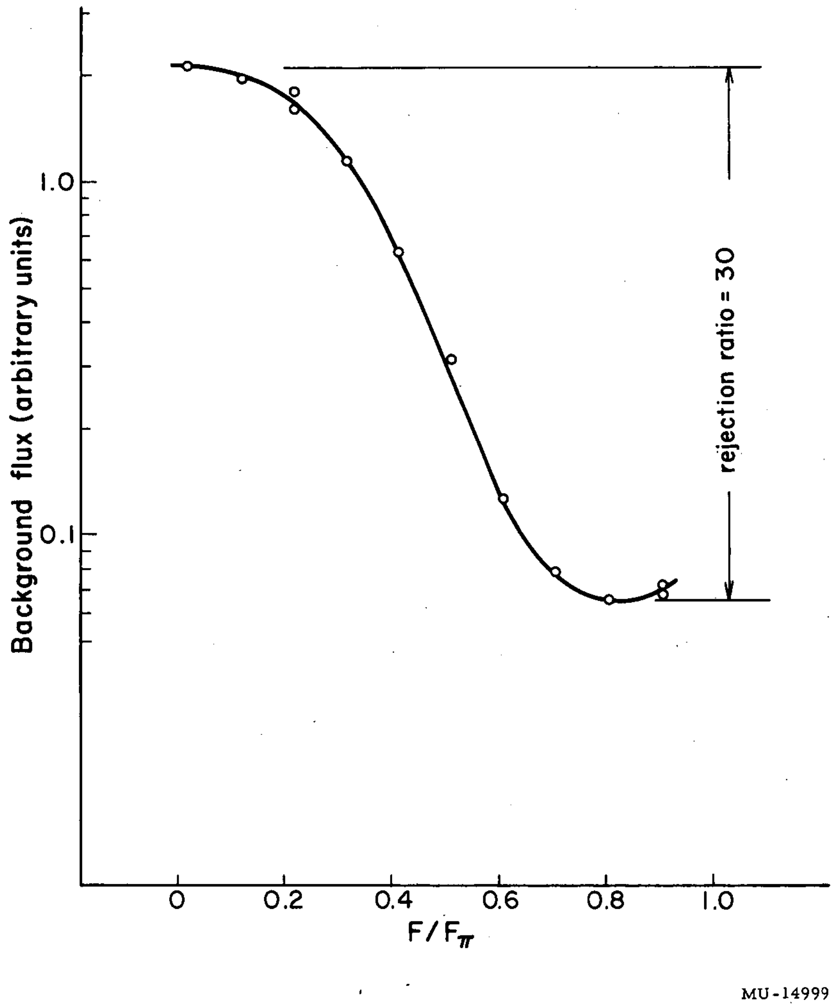

Fig. 5. Background flux vs F/F_π taken directly behind 3-in.-diam collimator ahead of Q2. V = 240 kv constant; H varied.

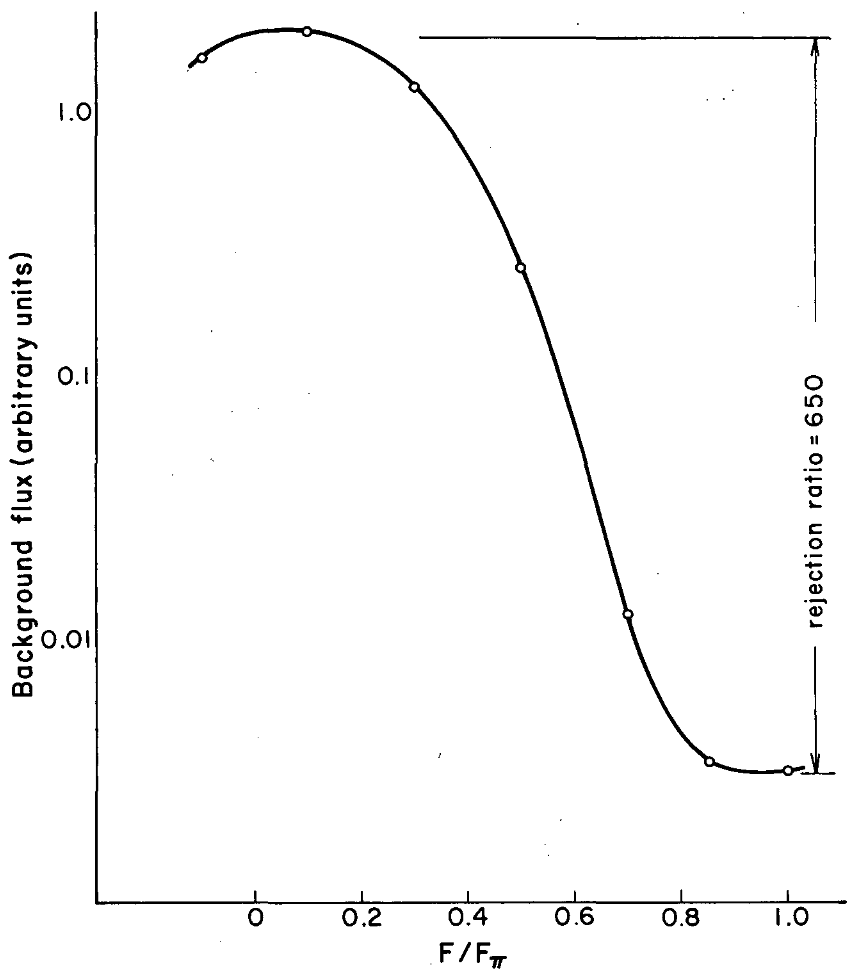

MU-15001

Fig. 6. Background flux vs F/F_π behind final collimator (1-in. vertical by 0.5-in. horizontal uranium-jawed slit). Collimator ahead of Q2 3.5 in. in diameter. Brass rod 0.75 in. in diam was installed on Q2 axis. V = 250 kv constant; H varied.

Most of the pions scattered from the outer conductor originate near the end of the spectrometer and arrive at Q2 with angles greater than 0.01 radian, that is, outside the acceptance aperture for full-momentum particles presented by the final collimator. Those originating before the end of the spectrometer may be deflected by outward forces in the spectrometer so as to arrive at Q2 with angles less than 0.01 radian and hence be accepted. Furthermore, the scattered pions in general have momenta less than maximum and some can, in spite of large entrance angles, arrive at the final aperture via anomalous trajectoris in Q2. Since these anomalous trajectoris cross or pass near the axis of Q2, they may be interrupted by an obstruction along the axis of Q2. Such an obstruction also favors transmission of desired particles over transmission of μ background, since the former is minimum on axis, while the latter is essentially uniform. It was found that a coaxial 3/4-inch-diameter brass rod stopping 8 inches short of the end of Q2 increased the rejection ratio about 30%.

In general, most of the background (~95%) ahead of Q2 has angles greater than 0.01 radian. This is demonstrated by the fact that the spatial distribution of the background at the focus of Q2 exhibits a minimum on axis and is concentrated in a region outside the main body of the transmitted beam (see Fig. 7).

The front-end optical system has the twofold purpose of dispersion removal and image formation. The bending angle in M1 is chosen so that, to first order, images formed at any momentum lie on the axis of the spectrometer. Q1 supplements focusing in the Bevatron field and in M1 so as to form a stigmatic central momentum image about 3 feet ahead of the end of the spectrometer.

Before the spectrometer was installed, the unobstructed image formed by the front-end optical system was studied (see Fig. 8). The width of the vertical profile is consistent with multiple scattering and finite source size. The excess horizontal width is presumably due to incomplete dispersion removal.

Comparing the integrated intensity in the unobstructed image--40×10^3 $\pi/10^{10}$ protons on target--with the integrated intensity entering C2--11×10^3 $\pi/10^{10}$ protons (see Fig. 9)--and correcting for π decay, one concludes that the transmission efficiency of the spectrometer and rear-end optical system is about 1/3 for pions. By insertion of additional scattering material at the various windows so as to simulate transmission of K mesons, the relative K/π transmission was found to be 0.8. Thus the over-all transmission efficiency for K mesons, neglecting decay, is about 25%. The relative $\overline{p}/\pi$ transmission is 0.4, giving an over-all $\overline{p}$ transmission efficiency of about 15%.

Using the relative efficiencies quoted above and correcting for decay and loss in the absorber ahead of the bubble chamber, one obtains K^-/π and $\overline{p}/\pi$ ratios at the target equal to 1:1000 and $1{:}2 \times 10^6$, respectively.

In Fig. 10 are curves that show how the intensities of the transmitted beam and of the background vary with steering-magnet current (M1). The former shows a peak and the latter shows a minimum at about the same magnet current. The increase in background for nonoptimum currents is presumably

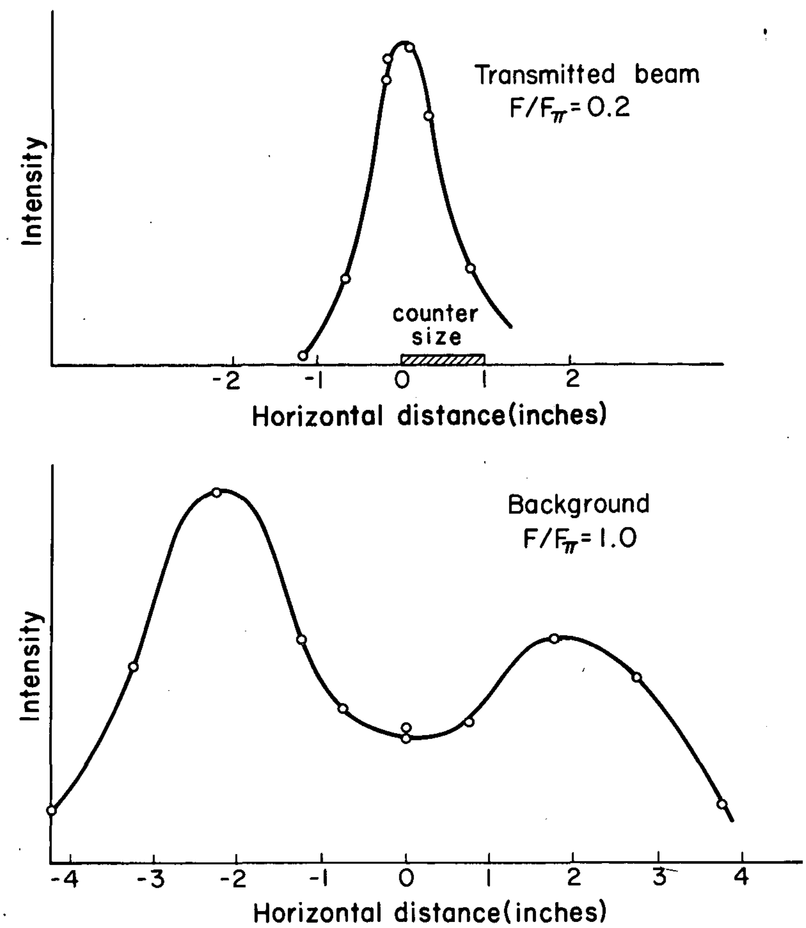

Fig. 7. Horizontal profiles of transmitted beam and of background 5 ft behind bubble chamber. Q2 was focused at this point with no final collimator. Rejection ratio with 1-in.-diameter counter was 1500.

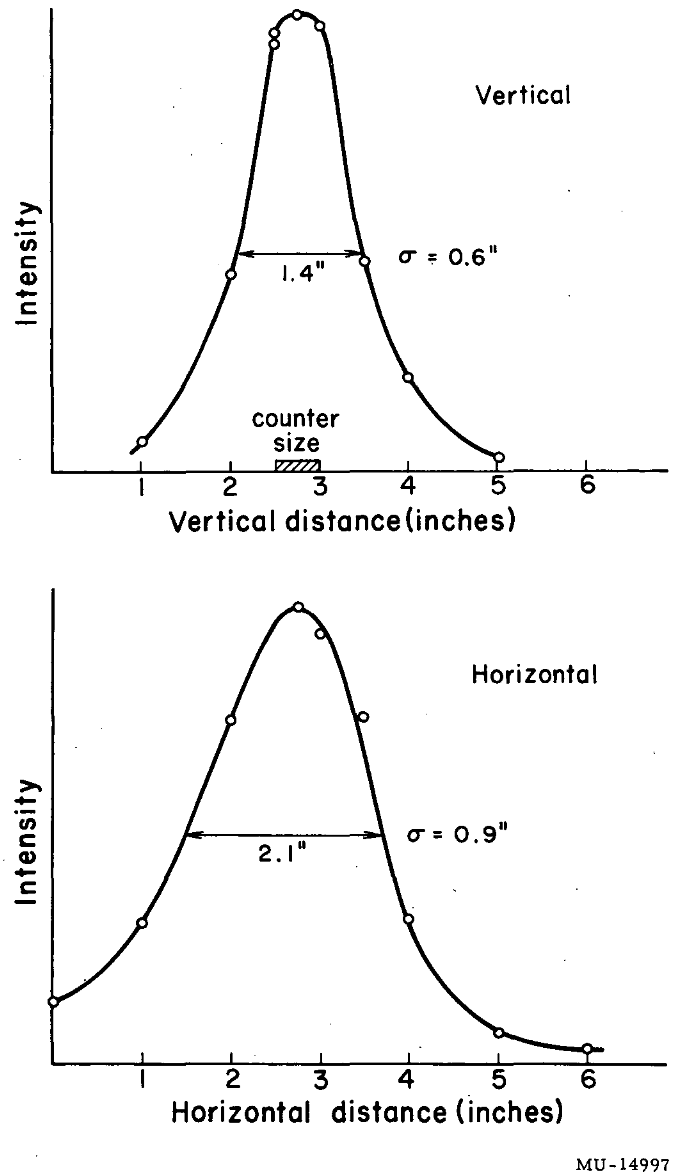

Fig. 8. Vertical and horizontal beam profiles at unobstructed image point 130 inches behind Q1 (spectrometer not installed). Integrated intensity was 4 x 10^4 $\pi/10^{10}$ protons on target.

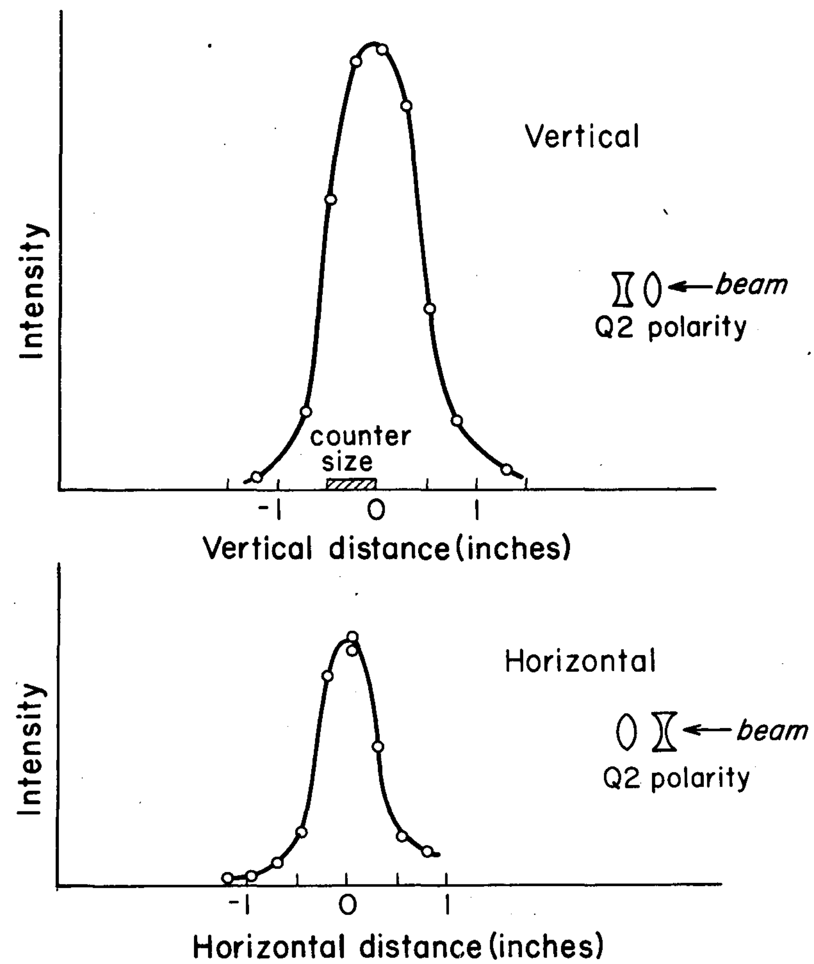

MU-15000

Fig. 9. Vertical and horizontal beam profiles at focus of Q2 (position of final collimator). $F/F_{\pi} = 0.2$. Total flux integrated over 1-in. vertical by 0.5-in. horizontal central area was 11×10^3 $\pi/10^{10}$ protons on target.

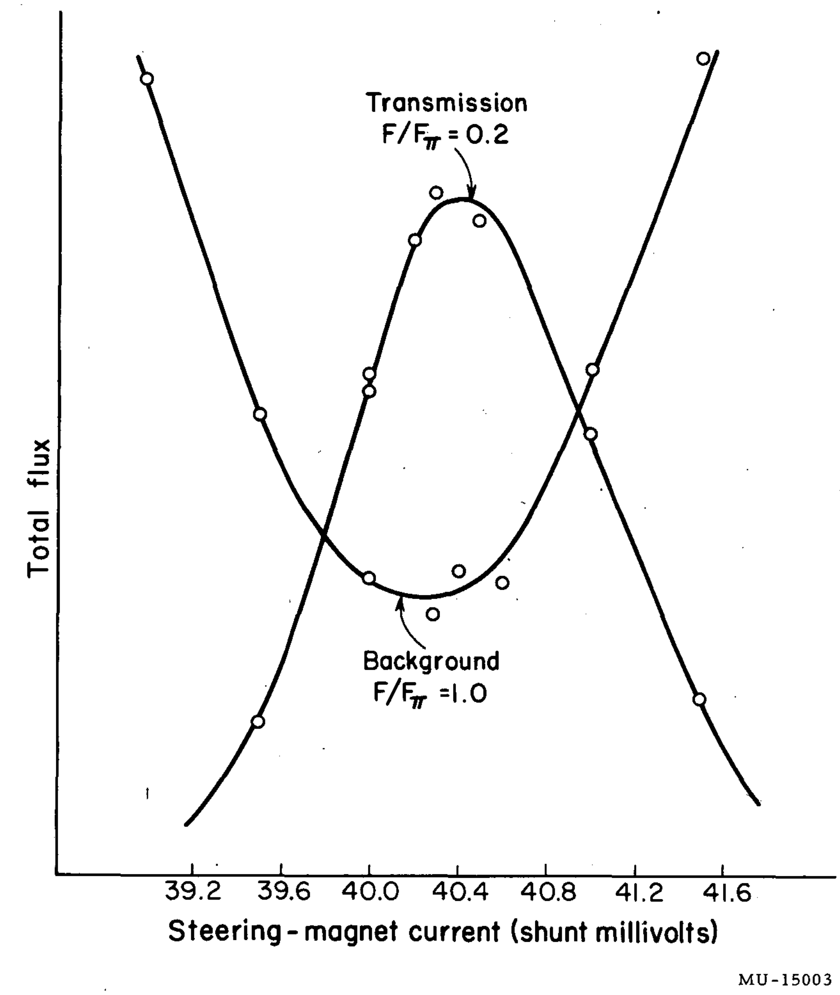

Fig. 10. Transmission and background vs steering-magnet current taken behind 1-in.-diam collimator at Q2 focus. Collimator ahead of Q2 3 in. in diameter.

due to an increase in the pion component scattered in from the outer conductor, which occurs when the beam is steered into the outer conductor. From these curves one can estimate the effect, in terms of transmission loss and background increase, resulting from magnet-current instability or varying Bevatron field. The latter may be important for beam spills prolonged more than 20 msec.

Analysis of this beam by means of an emulsion stack is described in the accompanying report.[3]

This work was done under the auspices of the U. S. Atomic Energy Commission.

[3] John N. Dyer, Analysis of the Bevatron K^- Beam by Means of an Emulsion Stack, UCRL-8364, July 1958.